Spectral normalization between Landsat-8/OLI, Landsat-7/ETM+ and CBERS-4/MUX bands through linear regression and spectral unmixing

Rennan F. B. Marujo[1], Leila Maria Garcia Fonseca[1], Thales Sehn Körting[1], Hugo do Nascimento Bendini[2]

[1]Image Processing Division – National Institute for Space Research (INPE)
São José dos Campos – SP, Brazil

[2]Remote Sensing Division – National Institute for Space Research (INPE)
São José dos Campos – SP, Brazil

{rennan.marujo, leila.fonseca, thales.korting, hugo.bendini}@inpe.br

Abstract. *Monitoring changes on Earth's surface is a difficult task commonly performed using multi-spectral remote sensing. The increasing availability of remote sensing platforms providing data makes multi-source approaches promising, since it can increase temporal revisit rate. However, Digital image processing techniques are needed to integrate the data, since sensors can be quite different in terms of acquisition characteristics. This work addresses the spectral normalizing of three medium spatial resolution sensors: Landsat-8/OLI, Landsat-7/ETM+ and CBERS-4/MUX, through linear regression and linear mixture model approaches. The results showed slight better results when using the linear regression approach.*

1. Introduction

Characterizing Earth's land cover and changes is essential to manage natural resources. Understanding the active processes and monitoring crops is vital for the ecosystems maintenance [Kuenzer et al., 2015]. Multi-spectral remote sensors estimate geo-biophysical properties using electromagnetic radiation as a medium of interaction [Choodarathnakara et al., 2012] and can help understand these changes [Boriah et al., 2008].

The Brazilian National Institute For Space Research (INPE) pioneered the free provision of medium resolution satellite data, releasing images with no cost of the second China Brazilian Earth Resources Satellite (CBERS-2) [Banskota et al., 2014]. The adoption of this policy encouraged the United States Geological Survey (USGS) to make the Landsat data available in 2008 [Woodcock et al., 2008; Banskota et al., 2014], which resulted in a greater amount of accesses and use of orbital images [Wulder et al., 2012].

Nowadays there are many satellite sensors obtaining information of Earth's surface. However, change detection methods normally use short remote sensing images time series, ranging from two to five images, and then they do not take advantage of full potential of historical series [Coppin et al., 2004]. This concept of having multiple images from different dates grouped in a single multi-dimensional array is known as an

image data cube. Integrate the spectral and spatial information with the time component provides rich information to detail the space variations along the time [Petitjean et al., 2012] and can provide pattern observations, which are not found in single time observations, such as trends and periodicities [Kuenzer et. al, 2015].

In many applications, e.g. crop monitoring [Steven et al., 2003] and change detection [Coppin et al., 2004], medium, or even high, spatial resolution images are required to provide the detailed information of the surface [Steven et al., 2003]. However, sensors revisit rate are long relative to plant active growth period [Steven et al., 2003] due to the trade-off between the spatial, radiometric and temporal resolution characteristics [Lefsky; Cohen, 2003]. Applications with multiple sensors were documented in the past years [Shimabukuro et al., 1991; Pohl; Van Genderen, 1998]. Therefore, the recent increasing number of onboard satellite sensors and its data availability has made these approaches more promising [Mousivand et al., 2015]. However, sensors heterogeneity concerning spectral, directional, radiometric and spatial characteristics must be treated in order to make the data compatible [Samain et al., 2006; Mousivand et al., 2015; Behling et al., 2016].

Samain et al. (2006) organized the multi-source heterogeneous aspects in four categories: spatial, temporal, spectral and directional. The optimum approach to deal with spatial differences between different sensors would be use multi-scale algorithms, which would use each sensor at its native spatial resolution. However, the complexity and processing cost of this approach is high. Resampling data to a common reference is more appropriate, even though this process may propagate loss of information, when data is resampled to the lowest spatial resolution, or introduce inaccurate measures, when resampling to the most refined resolution [Samain et al., 2006].

In relation to the temporal aspect, each onboard satellite sensor has its revisit time. Combine data from different sources and noise data can make the interval between acquisitions irregular. Similarly to the spatial aspect, the optimum approach would be to use each data on its native acquisition date. However, to facilitate image manipulation, several works in the literature supposes that there are few changes between images acquired close by each other. Based on that, an equidistant interval is adopted by performing operations, such as average or replacing, on those images and assuming it on close dates [Bendini et al., 2016; Vuolo et al., 2017].

Variations in spectral characteristics are harder to deal with, since different sensors with similar bandwidth present different responses to the same target [Trishchenko et al., 2002]. Based on that, values obtained from different sensors cannot be compared directly [Trishchenko et al., 2002]. These differences occur even if sensors have similar spectral bands, because the Specral Response Function (SRF) is specific for each sensor [Pinto et al., 2016]. In this context, Trishchenko et al. (2002) studied the effects of SRF on surface reflectance and NDVI measures comparing moderate resolution satellite sensors. They concluded that both measures are sensitive to the sensor's SRF and even for similar sensors a correction procedure is needed. Then, to combine data from different sensors it is necessary to equalize their SRFs, especially in the visible bands [Holden & Woodcock, 2016].

Bendini et al. (2016) used vegetation indices (EVI and NDVI) to derive phenological features of crops using filtered image time series and Random Forest

algorithm to classify agriculture. Holden & Woodcock (2016) used near-simultaneous Landsat-8 and Landsat-7 images to analyze consistency of both sensors surface reflection, since some spectral bands of Landsat-8 are narrow. The results showed that is necessary to normalize their spectral bands, since Landsat-8 visible bands (blue, green and red) are darker and near infrared band is brighter in the Landsat-7 satellite.

In this context, we proposed to test two methods to normalize spectral bands Landsat-8/OLI, Landsat-7/ETM+ and CBERS-4/MUX, through linear regression and linear mixture model approaches. The approaches are based on statistical [Samain et al., 2006; Bendini et al., 2016; Holden & Woodcock, 2016; Roy et al., 2016) and spectral information [Hubbard; Crowley, 2005; Gao et al., 2006; Zurita-Milla et al., 2008; Amorós-López et al., 2013].

2. Methodology

Figure 1 shows a diagram that describes the methodology to pre-process and spectrally normalize the images. The study area corresponds to the Path/Row 219/075 and 220/075 (WRS 2 – Worldwide Reference System 2), which intercept Landsat-7/ETM+ and Landsat-8/OLI images simultaneously, and also overlaps CBERS-4/MUX Path/Row 155/124 (CBERS WRS Path Row). Based on that, six cloud-free images were selected to perform the study composing an image data cube, i.e., two images from each sensor acquired in 04/07/2015 and 08/29/2015. In the pre-processing step, the images were converted to surface reflectance. Surface reflectance product for Landsat-7/ETM+ and Landsat-8/OLI images were acquired through USGS EROS Science Processing Architecture (ESPA) [USGS, 2017]. CBERS-4/MUX images were converted to top of atmosphere (Toa) radiance values and posteriorly to Toa reflectance, using methods proposed by Chander et al. (2009) and Pinto et al. (2016). Afterwards, Toa reflectance was converted to surface reflectance through atmospheric correction. The CBERS-4 images were radiometrically corrected and geometrically adjusted and refined by using control points and the SRTM 30m v. 2.1 digital elevation model (DEM) (Level 4). The atmospheric correction was proceeded using the 6S model (Second Simulation of a Satellite Signal in the Solar Spectrum) [VERMOTE et al. 1997].

After this pre-processing step, two spectral normalization methods were tested: linear regression and spectral unmixing. Both methods use a reference sensor and convert additional images to its pattern. The linear regression approach assumes that sensor bands relationship depends on illumination and observation geometry. It is based on the principle that calibrated and atmospherically corrected images from similar sensors are consistent and comparable, showing a low bias. Based on that, reflectance reference values are used to perform regression analysis with reflectance target values, resulting in gain and offset coefficients for each band, as illustrated on Figure 2. Steven et al. (2003) compared NDVI values from different instruments and obtained a strong linear relation between them. In this work, the linear regression coefficients were obtained considering the first date and, then were applied to images of second date, for each sensor.

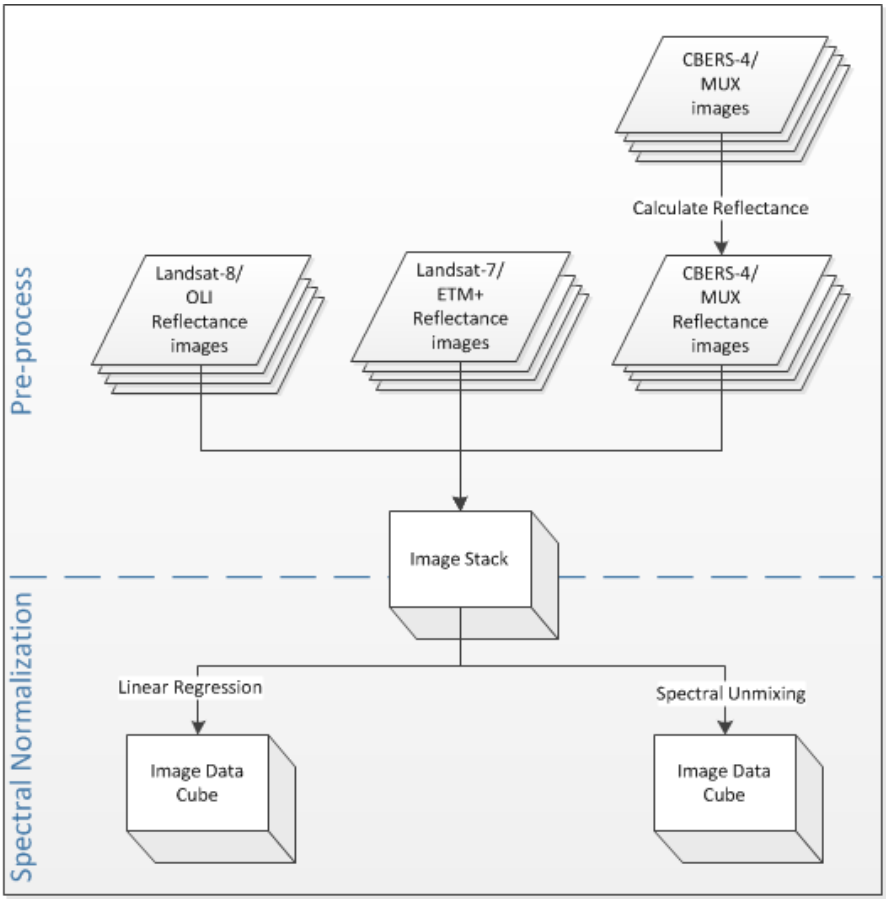

Figure 1. Methodology diagram.

The spectral approach is based on surface spectral signature restoration. It assumes that spectral reflectance can be decomposed in components, which are related to surface properties [SAMAIN et al., 2006]. Gao et al. (2006) and Zurita-Milla et al. (2008) combined moderate and medium spatial resolution sensors using this approach. One method that can be used in the spectral approach is spectral unmixing [Zurita-Milla et al., 2008]. In this method, endmembers for pre-determined classes, e.g. vegetation, soil and water/shadow, are used to transform the spectral image into a combination of class-fraction images through linear equations [Shimabukuro & Ponzoni, 2017]:

$$\rho_i = a \cdot veg_i + b \cdot soil_i + c \cdot shadow_i + e_i, \quad 1$$

where ρ_i is the pixel reflectance value in band i; a, b, and c are vegetation, soil and water/shadow proportion, respectively; veg_i, $soil_i$ and $shadow_i$ are vegetation, soil and water/shadow endmembers and e_i is the error in band i. Based on that, endmemembers obtained for a reference image can be applied in target images to construct a synthetic image [Gevaert; García-Haro, 2015], as illustrated on Figure 3. In this work, the endmembers for each class (vegetation, soil and water/shadow) were selected on each image, and used to obtain the class fraction images. Using Landsat-8/OLI as reference, the fraction images were used to the inversion of the process and generate synthetic images on different dates. The main advantage of this approach is that the class proportions instead of sensor spectral responses are used to restore each band.

Nevertheless, this approach is dependent on the endmember selection [Zurita-Milla et al., 2008].

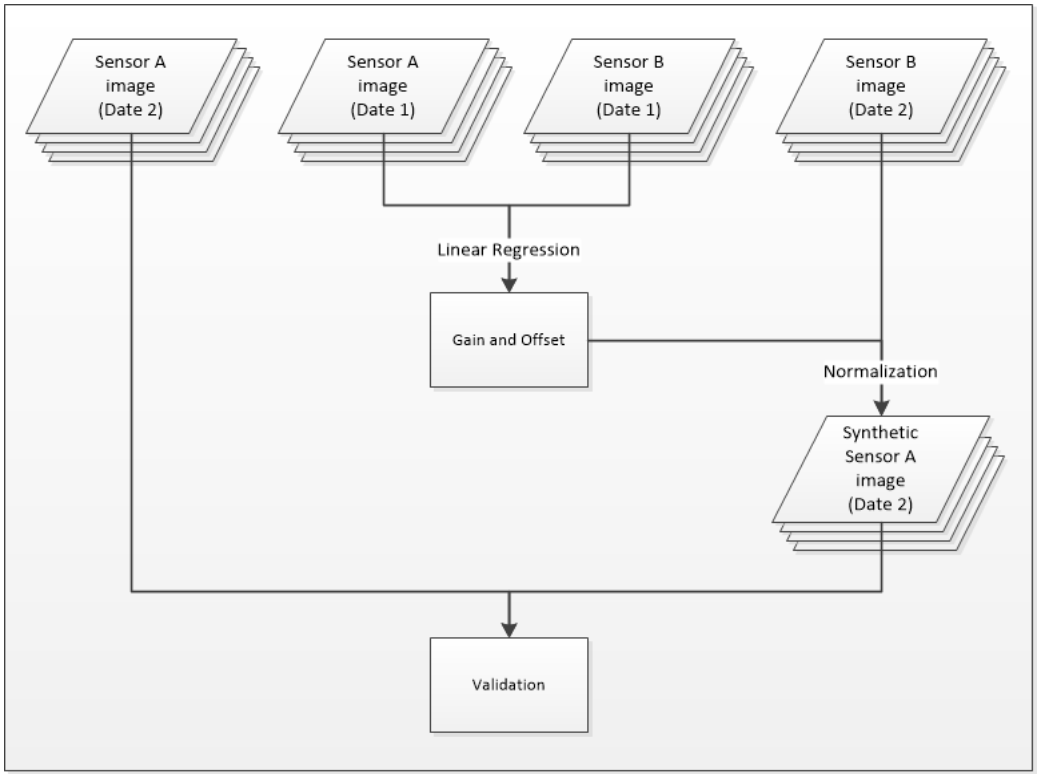

Figure 2. Linear regression spectral normalization diagram.

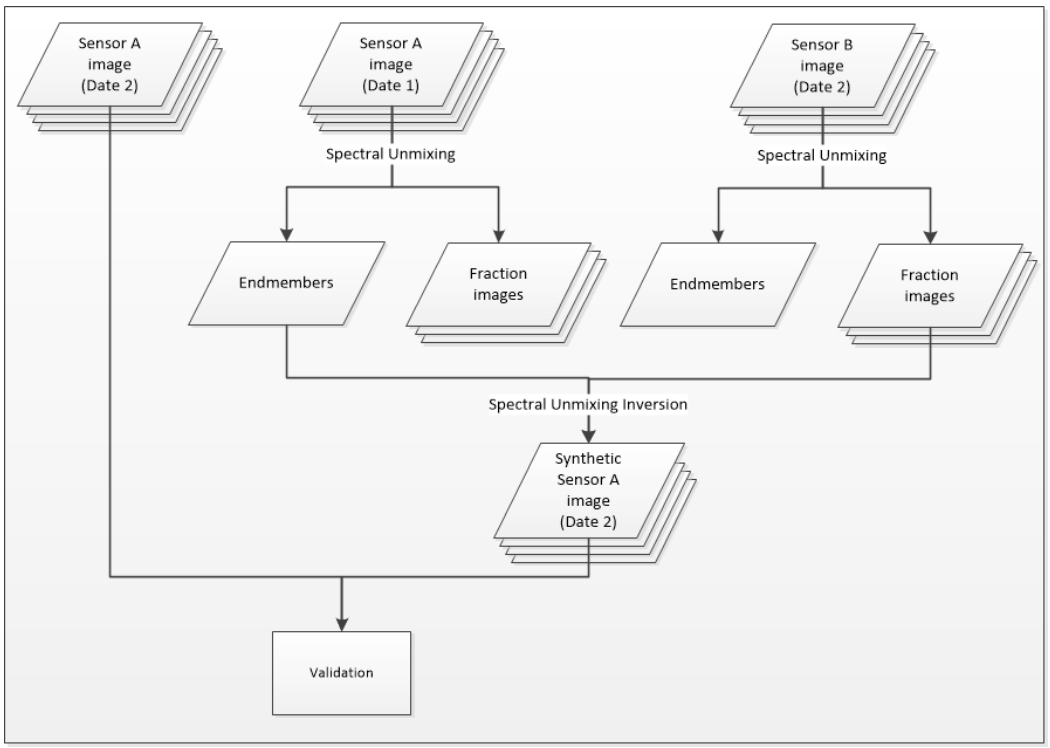

Figure 3. Spectral Unmixing normalization diagram.

3. Results and Discussion

Table 1 shows gain and offset values for each band obtained by regression method. They were used to transform Landsat-7/ETM+ and CBERS-4/MUX images into synthetic Landsat-8/OLI images, in the same date. Landsat-7/ETM+ was more consistent with Landsat-8/OLI than CBERS-4/MUX, as one can be observed in the gain values.

Table 1. Linear regression coefficients (gain and offset) for Landsat-8/OLI with CBERS-4/MUX and Landsat-8/OLI with Landsat-7/ETM+ in the blue, green, red and near infrared bands.

	Blue band		Green band		Red band		Nir band	
	Offset	Gain	Offset	Gain	Offset	Gain	Offset	Gain
L8_C4	184.78	0.69	106.13	0.89	28.04	1.02	209.25	1.28
L8_L7	-51.61	1.03	-24.89	1.05	-38.27	1.07	8.20	1.07

In the spectral unmixing experiment, Figure 4 shows endmember reflectance values for Lansat-8/OLI. Vegetation showed a greater response in the green band in comparison to the blue and red bands, with a peak in the near infrared, characteristic of vegetation targets [Jensen, 2007]. While soil class also had a typical exposed soil spectral response.

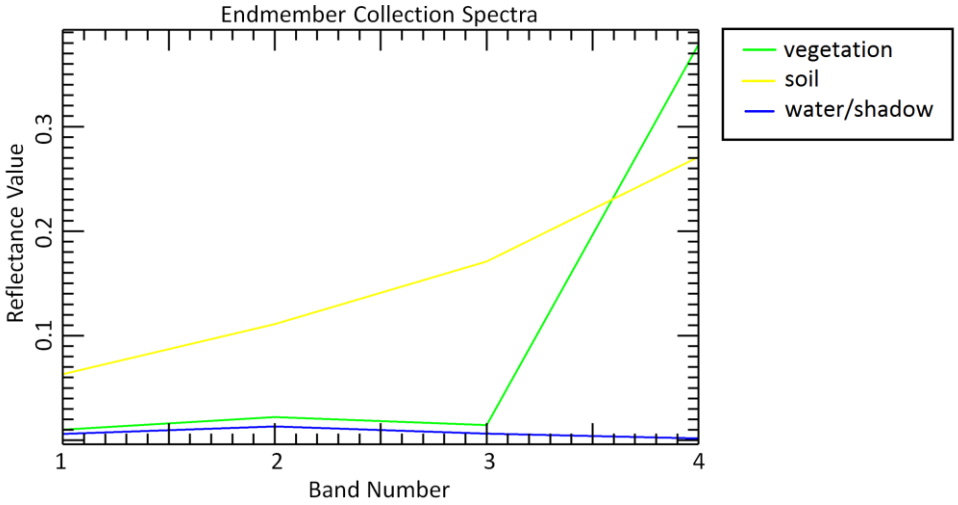

Figure 4. Spectral unmixing endmembers on Landsat-8/OLI sensor, collected for the classes vegetation (green curve), soil (yellow curve) and water/shadow (blue curve) in 4 multi-spectral band blue, green, red and near infra-red band.

We used Pearson's correlation to evaluate similarity among resulted images. Firstly we compared the synthetic images obtained through spectral unmixing to the reference images of both dates. Then, the synthetic images obtained throug linear regression for the second date were compared to the same reference images. The resulted Pearson's correlation coefficients are presented in Table 2.

Table 2. Pearson correlation coefficients obtained by normalizing, through linear spectral unmixing and through linear regression, Landsat-8/OLI (L8), Landsat-7/ETM+ (L7) and CBERS-4/MUX (C4) imagery from 04/07/2015 and 08/29/2015.

	Blue band	Green Band	Red Band	Nir Band
Unmixing L8 C4 (date 1)	0.77	0.82	0.84	0.89
Unmixing L8 C4 (date 2)	0.75	0.78	0.81	0.79
Unmixing L8 L7 (date 1)	0.88	0.94	0.96	0.94
Unmixing L8 L7 (date 2)	0.87	0.94	0.96	0.91
Regression L8 C4	0.82	0.90	0.95	0.95
Regression L8 L7	0.93	0.97	0.97	0.95

The results showed that shorter wavelength bands such as Blue and Green band are less inter-correlated than longer wavelength bands, such as Red and Near Infrared. This is probably due to atmospheric interference in shorter wavelength bands that was not completely suppressed by atmosphere correction [Jensen, 2007] as well as to the difference in the sensor spectral responses. Landsat-8/OLI and Landsat-7/ETM+ presented higher correlation than CBERS-4/MUX with Landsat-8/OLI. This similarity can be explained by the fact that Landsat-8/OLI is a continuity mission of Landsat-7/ETM+ and then is processed by similar methods. However, CBERS-4/MUX has potential to be used in time series analysis combined with Landsat 8 and Landst 7. Besides, linear regression spectral normalization approach presented slight better results than unmixed method.

4. Conclusion

In this work, we analyzed the spectral normalization of. Landsat-8/OLI, Landsat-7/ETM+ and CBERS-4/MUX based on linear regression and unmixing approaches in order to help overcome the lack of observations by merging multiple sensors data. The results showed that the used sensors have potential to be used in a multi-source, since the images were highly correlated. The correlation coefficients showed that shorter wavelength bands are less inter-correlated than longer wavelength bands and that Landsat-7/ETM+ is more correlated to Landsat-8/OLI than CBERS-4/MUX.

The spectral normalization of Landsat-8/OLI, Landsat-7/ETM+ and CBERS-4/MUX through linear regression spectral normalization approach presented slight better results than the unmixed method. Based on that, when spectrally normalizing Landsat-8/OLI, Landsat-7/ETM+ and CBERS-4/MUX sensors, the linear regression approach is recommended.

5. Acknowledgments

The authors would like to thank the Brazilian National Institute for Space Research (INPE) and FAPESP (Project #2014/08398-6 and Process #2016/08719-2), São Paulo Research Foundation for funding this research.

References

Amorós-López, J., Gómez-Chova, L., Alonso, L., Guanter, L., Zurita-Milla, R., Moreno, J., Camps-Valls, G. (2013) "Multitemporal fusion of Landsat/TM and ENVISAT/MERIS for crop monitoring". In: *International Journal of Applied Earth Observation and Geoinformation*, v. 23, n. 1, p. 132–141. Elsevier Inc.

Banskota, A., Kayastha, N., Falkowski, M. J., Wulder, M. A., Froese, R. E., White, J. C. (2014) "Forest monitoring using Landsat time series data: A review", In: *Canadian Journal of Remote Sensing*, v. 40, n. 5, p. 362–384. Taylor & Francis.

Behling, R., Roessner, S., Segl, K., Kleinschmit, B., Kaufmann, H. (2014) "Robust automated image co-registration of optical multi-sensor time series data: Database generation for multi-temporal landslide detection", In: *Remote Sensing*, v. 6, n. 3, p. 2572–2600. MPDI.

Behling, R., Roessner, S., Golovko, D., Kleinschmit, B. (2016) "Derivation of long-term spatiotemporal landslide activity - A multi-sensor time series approach", In: *Remote Sensing of Environment*, v. 186, p. 88–104. Elsevier Inc.

Bendini, H. N., Fonseca, L. M. G., Körting, T. S., Marujo, R. F. B. (2016) "Assessment of a Multi-Sensor Approach for Noise Removal on OLI / LANDSAT-8 Time Series Using MUX / CBERS-4 Data to Improve a Crop Classification Method Based on Phenological Features". Revista Brasileira de Cartografia. 2017. (in press)

Boriah, S., Kumar, V., Steinbach, M., Potter, C., Klooster, S. (2008) "Land cover change detection". In: P*roceeding of the 14th ACM SIGKDD international conference on Knowledge discovery and data mining – KDD*, v. 8. New York, USA: ACM Press.

Chander, G., Markham, B. L., Helder, D. L. (2009) "Summary of current radiometric calibration coefficients for Landsat MSS, TM, ETM+, and EO-1 ALI sensors", In:. *Remote Sensing of Environment*, v. 113, n. 5, p. 893–903. Elsevier Inc.

Choodarathnakara, A. L., Kumar, T., Shivaprakash, K., Patil, C. (2012) "Soft Classification Techniques for RS Data". In: *International Journal of Computer Science Engineering and Technology*, v. 2, n. 11, p. 1468–1471. Springer.

Coppin, P., Jonckheere, I., Nackaerts, K., Muys, B., Lambin, E. (2004) "Digital change detection methods in ecosystem monitoring: a review". In: *International Journal of Remote Sensing*, v. 25, n. 9, p. 1565–1596. . Taylor & Francis.

Gao, F., Masek, J., Schwaller, M., Hall, F. (2006) "On the blending of the landsat and MODIS surface reflectance: Predicting daily landsat surface reflectance". In: *IEEE Transactions on Geoscience and Remote Sensing*, v. 44, n. 8, p. 2207–2218. IEEE Computer Society.

Gevaert, C. M., García-Haro, F. J. (2015) "A comparison of STARFM and an unmixing-based algorithm for Landsat and MODIS data fusion". In: *Remote Sensing of Environment*, v. 156, p. 34–44. Elsevier Inc.

Holden, C. E., Woodcock, C. E. (2016) "An analysis of Landsat 7 and Landsat 8 underflight data and the implications for time series investigations". In: *Remote Sensing of Environment*, v. 185, p. 16–36. Elsevier Inc.

Hubbard, B. E., Crowley, J. K. (2005) “Mineral mapping on the Chilean-Bolivian Altiplano using co-orbital ALI, ASTER and Hyperion imagery: Data dimensionality issues and solutions”. In: *Remote Sensing of Environment*, v. 99, n. 1-2, p. 173–186. Elsevier Inc.

Jensen, J. (2007), Remote Sensing of the Environment: An Earth Resource Perspective, New Jersey: Pearson Prentice Hall.

Kuenzer, C., Dech, S., Wagner, W. (2015), “Remote Sensing Time Series: Revealing Land Surface Dynamics”, In: *Remote Sensing and Digital Image Processing*, v. 22. Springer International.

Lefsky, M. A., Cohen, W. B. (2003) “Selection of Remotely Sensed Data”, In: *Remote Sensing of Forest Environments*. Norwell Massachusetts, USA: p. 13–46. Academic Press.

Mousivand, A., Menenti, M., Gorte, B., Verhoef, W. (2015) “Multi-temporal, multi-sensor retrieval of terrestrial vegetation properties from spectral-directional radiometric data”, *Remote Sensing of Environment*, v. 158, p. 311–330. Elsevier Inc.

Petitjean, F., Inglada, J., Gançarski, P. (2012) “Satellite image time series analysis under time warping”, In: *IEEE Transactions on Geoscience and Remote Sensing*, v. 50, n. 8, p. 3081–3095. IEEE Computer Society.

Pinto, C., Ponzoni, F., Castro, R., Leigh, L., Mishra, N., Aaron, D., Helder, D. (2016) “First in-Flight Radiometric Calibration of MUX and WFI on-Board CBERS-4”, In: *Remote Sensing*, v. 8, n. 5, p. 405. MPDI.

Pohl, C., Van Genderen, J. L. (1998) “Review article Multisensor image fusion in remote sensing: Concepts, methods and applications”, *International Journal of Remote Sensing*, v. 19, n. 5, p. 823–854. Taylor & Francis.

Roy, D. P., Zhang, H. K., Ju, J., Gomez-Dans, J. L., Lewis, P. E., Schaaf, C. B., Sun, Q., Li, J., Huang, H., Kovalskyy, V. (2016) “A general method to normalize Landsat reflectance data to nadir BRDF adjusted reflectance”, In: *Remote Sensing of Environment*, v. 176, p. 255–271. Elsevier Inc.

Samain, O.; Geiger, B.; Roujean, J. L. (2006) “Spectral normalization and fusion of optical sensors for the retrieval of BRDF and albedo: Application to VEGETATION, MODIS, and MERIS data sets”, In: *IEEE Transactions on Geoscience and Remote Sensing*, v. 44, n. 11, p. 3166–3178. IEEE Computer Society.

Shimabukuro, Y. E., Ponzoni, F. J. (2017) “Modelo Linear e Aplicações”. São Paulo: Oficina de Textos, 128 p. Oficina de Textos.

Shimabukuro, Y. E., Santos, J. R., Rernandez Filho, P., Lee, D. C. L. (1991) “Avaliação conjuntural da técnica de abordagem multisensor para o monitoramento da vegetação do brasil”, In: *Simpósio Latino Americano de Percepcion Remota*. 13 p. Cuzco, Peru. SELPER.

Steven, M. D., Malthus, T. J., Baret, F., Xu, H., Chopping, M. J. (2003) “Intercalibration of vegetation indices from different sensor systems”, In: *Remote Sensing of Environment*, v. 88, n. 4, p. 412–422.

Trishchenko, A. P., Cihlar, J., Li, Z. (2002) “Effects of spectral response function on surface reflectance and NDVI measured with moderate resolution satellite sensors”, In: *Remote Sensing of Environment*, v. 81, n. 1, p. 1–18. Elsevier Inc.

USGS (2017). “User Guide: Earth Resources Observation and Science (EROS) Center Science Processing Architecture (ESPA) on demand interface”. Sioux Falls.

Vermote, E.; Justice, C.; Claverie, M.; Franch, B. (2016) “Preliminary analysis of the performance of the Landsat 8/OLI land surface reflectance product”, In: *Remote Sensing of Environment*, v. 185, n. 1, p. 46 – 56. Elsevier Inc.

Vuolo, F., Ng, W.-T., Atzberger, C. (2017) “Smoothing and gap-filling of high resolution multi-spectral time series: Example of Landsat data”. *International Journal of Applied Earth Observation and Geoinformation*, v. 57, p. 202–213. Elsevier.

Woodcock, C. E., Allen, R., Anderson, M., Belward, A., Bindschadler, R., Cohen, W., Gao, F., Goward, S. N., Helder, D., Helmer, E. H., Nemani, R., Oreopoulos, L., Schott, J., Thenkabail, P. S., Vermote, E. F., Vogelmann, J. E., Wulder, M. A., Wynne, R. H. (2008) “Free Access to Landsat Imagery”, In: *Science*, v. 320, n. May, p. 1011–1012.

Wulder, M. A., Masek, J. G., Cohen, W. B., Loveland, T. R., Woodcock, C. E. (2012) “Opening the archive: How free data has enabled the science and monitoring promise of Landsat”, In: *Remote Sensing of Environment*, v. 122, p. 2–10. Elsevier Inc.

Zurita-Milla, R., Clevers, J. G. P. W., Schaepman, M. E. (2008) “Unmixing-based landsat TM and MERIS FR data fusion”, In: *IEEE Geoscience and Remote Sensing Letters*, v. 5, n. 3, p. 453–457. IEEE Computer Society.